

# Impact of scalar NSI with off-diagonal parameters at DUNE and P2SO

Sambit Kumar Pusty,<sup>1,\*</sup> Rudra Majhi,<sup>2,†</sup> Dinesh Kumar Singha,<sup>1,‡</sup> Monojit Ghosh,<sup>3,§</sup> and Rukmani Mohanta<sup>1,¶</sup>

<sup>1</sup>*School of Physics, University of Hyderabad, Hyderabad - 500046, India*

<sup>2</sup>*Nabarangpur College, Nabarangpur - 764063, Odisha, India*

<sup>3</sup>*Center of Excellence for Advanced Materials and Sensing Devices, Ruder Bošković Institute, 10000 Zagreb, Croatia*

## Abstract

In this paper, we studied the impact of the off-diagonal SNSI parameters in the future long-baseline neutrino oscillation experiments DUNE and P2SO. In our analysis, we found that the sensitivities of these experiments altered in a very non-trivial way due to the presence of these parameters. Depending on the values of these parameters, they can either completely mimic the standard scenario or can wash out their CP sensitivity. For large values of parameters  $\eta_{e\mu}$  and  $\eta_{e\tau}$ , we obtained larger mass ordering and octant sensitivities as compared to the standard three flavour scenario. For the parameter  $\eta_{\mu\tau}$ , the mass ordering sensitivity and the precision of  $\Delta m_{31}^2$  deteriorated compared to the standard scenario. Our results also showed that the sensitivities significantly influenced by the phases of the off-diagonal parameters.

---

\* pustysambit@gmail.com

† rudra.majhi95@gmail.com

‡ dinesh.sin.187@gmail.com

§ mghosh@irb.hr

¶ rmisp@uohyd.ac.in

## I. INTRODUCTION

The origin of small and non-zero neutrino masses inferred from various neutrino oscillation experiments remains so far as a mystery and thus provides an ideal platform to explore physics beyond the Standard Model (BSM). Over the past few decades, there has been remarkable advancement in the precise determination of various neutrino oscillation parameters. Among these parameters, the mass-squared differences and the mixing angles, except  $\theta_{23}$ , are measured with a precision of a few percent. On the other hand, the CP violating phase  $\delta_{CP}$  so far remains unascertained. Additionally, the issues related to the sign of  $\Delta m_{31}^2$ , the so-called mass ordering problem and the octant of  $\theta_{23}$  are yet to be resolved [1, 2]. Despite these unknowns, the neutrino sector can be regarded as a means to probe new and unexplored areas of BSM physics. Neutrinos originating from various sources, such as the atmosphere, accelerators, and reactors, have been studied extensively in various oscillation experiments. In particular, long-baseline experiments have proven to be highly effective for the precise determination of the oscillation parameters due to the presence of matter effect. Consequently, these experiments provide an excellent opportunity to probe various BSM frameworks, which can induce sub-leading effects in the neutrino oscillation phenomena.

Various sub-dominant repercussions of BSM Physics, such as Non-Standard Interactions (NSIs) [3–7], Lorentz Invariance Violation (LIV) [8–11], Long Range Force (LRF) [12–14], Neutrino Decay [15–19], Decoherence [20–23], etc., have been studied extensively in the context of long-baseline neutrino oscillation experiments. Within the realm of BSM physics, the NSI of neutrinos emerges as a notable and well motivated phenomenon. Various experiments have already delved into NSI signals, associated with charge current (CC) [24] as well as neutral current (NC) [25] interactions. It should be emphasized that, the CC and NC NSIs are mediated through vector fields. Corresponding effects of NC-NSI appeared as a potential term in the Hamiltonian for neutrino oscillation, whereas CC NSI modifies the neutrino flavour states in the time evolution equation. More generally, the CC-NSI affects the production and detection mechanisms of neutrinos at the source and detector, while the NC-NSI affects the propagation of neutrinos between the source and detector. On the other hand, if the NSIs are mediated by a scalar, the corresponding interactions contribute as a correction to the neutrino mass matrix rather than the matter potential. Consequently, the effect of scalar NSI becomes energy independent, while the vector one scales linearly with neutrino energy, which leads to significantly different phenomenological consequences in neutrino oscillation experiments. Recent studies elaborately discuss the NSI of neutrinos mediated by a light scalar particle [26–42]. This newly emerged interaction is known as Scalar NSI (SNSI). Apart from providing additional contribution to the neutrino mass, SNSI can also worsen the determination of the unknowns in the neutrino sector. The effect of SNSI can be parameterised as a complex matrix with complex off-diagonal parameters and real diagonal parameters. Several articles have discussed the effects of diagonal and off-diagonal parameters at various long-baseline experiments, such as DUNE [28, 31–34, 37, 39, 40],

T2HK[32, 39], T2HKK [32, 39], ESSnuSB [29, 38] and P2SO [36].

In one of our recent studies, we have explored the impact of the diagonal SNSI parameters in the context of DUNE and P2SO [36]. In our work, we have shown that the atmospheric mass square difference  $\Delta m_{31}^2$  plays a non-trivial role when one tries to put bounds on some of the diagonal SNSI parameters, and CP sensitivities of these experiments are lost for a particular value of the SNSI parameter  $\eta_{ee}$ . For the later, we derived an analytical expression and showed this explicitly. In this paper, our aim is to extend that study by including the off-diagonal SNSI parameters. Unlike the diagonal parameters, the off-diagonal parameters are complex in nature and hence, there are additional phases associated with them. The main goal of this paper is to understand how these additional phases impact when (i) one tries to put bounds on the SNSI parameters and (ii) when one tries to measure the sensitivities to the standard parameters. It will be interesting to see if the conclusions we obtained for the diagonal SNSI parameters remain the same for the off-diagonal NSI parameters. Further, we also expect to observe a significant change in the CP sensitivity, as the presence of the new phases can impact the sensitivity of the standard CP phase  $\delta_{CP}$  as discussed in the Appendix C of Ref. [36].

The paper is organized as follows. The next section will be on the theoretical background of SNSI parameters. Simulation details and experimental configuration will be discussed in the section III. Then in section IV, we will present our results and findings on SNSI. Finally, we will conclude the paper with a summary in section V.

## II. THEORETICAL FRAMEWORK

The Lagrangian corresponding to the simplest model that describes SNSI, can be expressed as [26, 37],

$$\mathcal{L} = \bar{\nu}_\alpha (i\gamma^\mu \partial_\mu - M_{\alpha\beta}) \nu_\beta - (y_\nu)_{\alpha\beta} \bar{\nu}_\alpha \nu_\beta \phi - y_f \bar{f} f \phi - \frac{1}{2} (\partial_\mu \phi)^2 - \frac{m_\phi^2}{2} \phi^2 \quad (1)$$

where  $y_f$  is the Yukawa coupling of the scalar mediator  $\phi$  with fermion  $f$ ,  $y_\nu$  is the Yukawa coupling of the scalar mediator with the neutrinos  $\nu$ , and  $m_\phi$  is the mass of the scalar mediator. Here  $\alpha$  and  $\beta$  are the flavour index of the leptons. Without delving into the details of model building aspects, we presume that the neutrinos interact with the fermions in a non-standard way through a scalar mediator. The corresponding effective Lagrangian can be written as,

$$\mathcal{L}_{\text{eff}} = \frac{y_{\alpha\beta} y_f}{m_\phi^2} (\bar{\nu}_\alpha \nu_\beta) (\bar{f} f). \quad (2)$$

The Dirac equation in the presence of SNSI can be written as [26]:

$$\bar{\nu}_\alpha \left[ i\partial_\mu \gamma^\mu + \left( M_{\alpha\beta} + \frac{\sum_f N_f y_{\alpha\beta} y_f}{m_\phi^2} \right) \right] \nu_\beta = 0, \quad (3)$$

where  $M_{\beta\alpha}$  is the Dirac mass matrix of the neutrinos and  $N_f$  is the number density of fermion  $f$ . Therefore, we note that the effect of SNSI appears as a correction term within the neutrino mass matrix. This correction can be characterized as

$$\delta M = \sqrt{|\Delta m_{31}^2|} \begin{pmatrix} \eta_{ee} & \eta_{e\mu} & \eta_{e\tau} \\ \eta_{\mu e} & \eta_{\mu\mu} & \eta_{\mu\tau} \\ \eta_{\tau e} & \eta_{\tau\mu} & \eta_{\tau\tau} \end{pmatrix}, \quad (4)$$

where we have considered  $\eta_{\alpha\beta}$  as SNSI parameters. In order to make SNSI parameter  $\eta_{\alpha\beta}$  dimensionless, we scale the magnitude of  $\delta M$  relative to  $\sqrt{|\Delta m_{31}^2|}$ , where  $\Delta m_{31}^2 = m_3^2 - m_1^2$  is the atmospheric mass square difference. Comparing Eqs. 3 and 4, one can write

$$\eta_{\alpha\beta} = \frac{1}{m_\phi^2 \sqrt{|\Delta m_{31}^2|}} \sum_f N_f y_f y_{\alpha\beta}. \quad (5)$$

In order to have  $\delta M$  to be Hermitian, we have considered the diagonal elements  $\eta_{\beta\beta}$  as real and the off-diagonal elements  $\eta_{\alpha\beta}$  with  $\alpha \neq \beta$  as complex. As mentioned in the introduction, in this work we will focus only on the off-diagonal elements, which we parametrize as  $\eta_{\alpha\beta} = |\eta_{\alpha\beta}| e^{i\phi_{\alpha\beta}}$ . From Eq. 5, it is clear that the SNSI parameters depend on the matter density<sup>1</sup>. As a result, care should be taken while comparing the values of  $\eta_{\alpha\beta}$  in accordance with the matter density profile of different experiments. For P2SO and DUNE experiments, matter density are nearly equal and the results of  $\eta$  can be comparable.

At this point, it is important to comment on the present bounds on the Yukawa couplings and the mass of the scalar mediator and how our results can be correlated with these bounds. A detailed discussion on this topic is available in Refs. [36] and [38]. In summary, the bounds obtained in our analysis are model independent. However, the effective couplings  $\eta_{\alpha\beta}$  receive constraints from the experiments that are sensitive to neutrino-electron and/or neutrino-nucleon elastic scattering [43]. These bounds would also be expected to be model independent. As discussed in Ref. [37], this scenario is expected to be constrained from Borexino data on solar neutrinos and data from SN1987A. A discussion on constraints on SNSI parameters from solar and a combination of solar and reactor experiments is available in Ref. [41]. Finally, it has been shown in Ref. [43] that the same values of the couplings satisfy a wide range of mediator mass. Therefore, there will not be a direct correlation between the bounds of the SNSI parameters obtained from scattering experiments and the neutrino oscillation experiments.

The effective Hamiltonian of neutrino oscillation considering scalar NSI can be written as

$$H = E_\nu + \frac{MM^\dagger}{2E_\nu} + V, \quad (6)$$

---

<sup>1</sup> Note that NSI mediated by a vector field (VNSI) also depends on the matter density. However, for VNSI, the matter term appears with energy  $E$ . To understand the separation of VNSI from SNSI at the Hamiltonian and probability level we refer to Appendix A of Ref. [36]

where  $E_\nu$  is the energy of the neutrinos,  $V = \text{diag}(\sqrt{2}G_F N_e, 0, 0)$  is the standard matter potential with  $G_F$  is the Fermi constant and  $N_e$  is the electron number density. In this case, the term  $M$  becomes

$$\begin{aligned} M &= U \text{diag}(m_1, m_2, m_3) U^\dagger + \delta M \\ &= U \text{diag} \left( m_1, \sqrt{m_1^2 + \Delta m_{21}^2}, \sqrt{m_1^2 + \Delta m_{31}^2} \right) U^\dagger + \delta M, \end{aligned} \quad (7)$$

where we have assumed normal ordering of the neutrino masses i.e.,  $m_3 \gg m_2 > m_1$ . Here  $\Delta m_{21}^2 = m_2^2 - m_1^2$  is the solar mass squared difference and  $U$  is the standard PMNS matrix. Neutrino oscillation probabilities in presence of SNSI can be calculated by diagonalizing Eq. 6. The neutrino oscillation probabilities will depend on the SNSI parameter as well as on the lightest neutrino mass  $m_1$ .

### III. SIMULATION DETAILS

In this section, we will discuss the details of the experimental configuration as well as the simulation methods used in this analysis. We have considered two long-baseline experiments DUNE and P2SO. The detailed configurations are outlined below.

#### P2SO

The Protvino to Super-ORCA (P2SO) is an upcoming long-baseline experiment. In this setup, neutrinos will be generated at a U-70 synchrotron located in Protvino, Russia, and will travel to a detector positioned 2595 km away in the Mediterranean Sea, 40 km offshore Toulon, France. Detailed configuration information for the P2SO experiment can be found in Refs. [44–46].

The accelerator is designed to produce a 450 KW beam, equating to  $4 \times 10^{20}$  protons on target annually for the P2SO configuration. Notably, the Super-ORCA detector employs a density that is ten times greater than the ORCA detector. The energy window for the P2SO experiment spans from 0.2 GeV to 10 GeV. The total run period considered is six years, divided into three years each for neutrino and antineutrino modes.

#### DUNE

DUNE is an upcoming long-baseline neutrino oscillation experiment situated at Fermilab in the USA. We have used the official GLOBES files corresponding to the technical design report (TDR) [47] for simulating the DUNE experiment. The DUNE experiment operates over a broad range of neutrino energies, corresponding to a high beam power of 1.2 MW.

The near detector is located at Fermilab, and the far detector is 40 kt liquid argon time projection chamber (LArTPC) situated in South Dakota.

In our analysis, we consider the total run-time for DUNE to be 13 years, comprising 6.5 years in neutrino mode and 6.5 years in antineutrino mode. This duration corresponds to an accumulation of  $1.1 \times 10^{21}$  protons on target (POT) per year.

For simulation, we are using GLoBES software package [48, 49]. In order to implement SNSI, we have modified the probability engine of GLoBES. We estimate the sensitivity in terms of  $\chi^2$  analysis. We use the Poisson log-likelihood and assume that it is  $\chi^2$ -distributed:

$$\chi_{\text{stat}}^2 = 2 \sum_{i=1}^n \left[ N_i^{\text{test}} - N_i^{\text{true}} - N_i^{\text{true}} \log \left( \frac{N_i^{\text{test}}}{N_i^{\text{true}}} \right) \right], \quad (8)$$

where  $N^{\text{test}}$  and  $N^{\text{true}}$  are the number of events in the test and true spectra respectively, and  $n$  is the number of energy bins. The systematic error is incorporated by the method of pull [50, 51]. The values of the oscillation parameters are taken from NuFit 5.2 and are listed in Tab. I. In our calculation, we have minimized over the parameters  $\theta_{23}$ ,  $\Delta m_{31}^2$ ,  $\delta_{CP}$  and the phases of the complex SNSI parameters appropriately. We present our results for the normal ordering of the neutrino masses and taken  $m_1 = 10^{-5}$  eV. Throughout our analysis, we will consider only one SNSI parameter at a time.

Parameters	Best fit value $\pm 1\sigma$	$3\sigma$
$\sin^2 \theta_{12}$	$0.303_{-0.012}^{+0.012}$	$0.270 \rightarrow 0.341$
$\sin^2 \theta_{13}$	$0.02225_{-0.00059}^{+0.00056}$	$0.02052 \rightarrow 0.02398$
$\sin^2 \theta_{23}$	$0.451_{-0.016}^{+0.019}$	$0.408 \rightarrow 0.603$
$\delta_{CP}/^\circ$	$232_{-0.26}^{+0.36}$	$144 \rightarrow 350$
$\Delta m_{21}^2/10^{-5} \text{ eV}^2$	$7.41_{-0.20}^{+0.21}$	$6.82 \rightarrow 8.03$
$\Delta m_{31}^2/10^{-3} \text{ eV}^2$	$+2.507_{-0.027}^{+0.026}$	$+2.427 \rightarrow +2.590$

TABLE I: Oscillation parameters values with their  $1\sigma$  and  $3\sigma$  regions as mentioned in NuFIT 5.2. [1]

#### IV. RESULTS

In this section, we will show the impact of off-diagonal SNSI parameters on the sensitivities of P2SO and DUNE. First, we will estimate the capability of these experiments to put bounds on the SNSI parameters by taking the standard scenario in true and the SNSI in test and then we will study how the sensitivities corresponding to the standard oscillation parameters are altered in the presence of off-diagonal SNSI parameters by taking SNSI in both true and test.

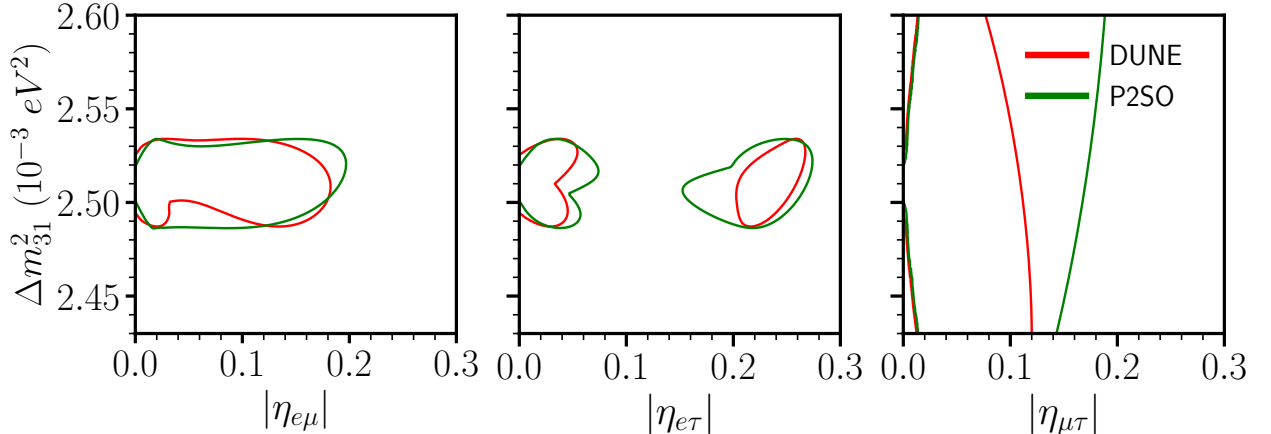


FIG. 1: Allowed parameter space between  $|\eta_{\alpha\beta}|$  and  $\Delta m_{31}^2$  at 90% C.L. for DUNE and P2SO experiment.

### A. Sensitivity limits on SNSI parameters

In Ref. [36], we have seen that the parameter  $\Delta m_{31}^2$  plays a non-trivial role in constraining the diagonal SNSI parameters. To understand the situation for the off-diagonal SNSI parameters, in Fig. 1, we have plotted the 90% C.L. contours in  $|\eta_{\alpha\beta}|$  vs  $\Delta m_{31}^2$  plane. The left/middle/right panel is for  $\eta_{e\mu}/\eta_{e\tau}/\eta_{\mu\tau}$ . In each panel, the red contour is for DUNE and the green contour is for P2SO. The y-axis in the figure shows the current  $3\sigma$  C.L. allowed region of  $\Delta m_{31}^2$ . From this figure, we observed that for  $\eta_{e\mu}$  and  $\eta_{e\tau}$ , SNSI can be fitted with the standard scenario with a value of  $\Delta m_{31}^2$  lying within its  $3\sigma$  region. This is evident from the close nature of the contours. This is in sharp contrast with the diagonal parameters  $\eta_{\mu\mu}$  and  $\eta_{\tau\tau}$ , where the standard case can also be fitted with SNSI with a value of  $\Delta m_{31}^2$  outside its  $3\sigma$  allowed values as shown in Ref. [36]. This means for the off-diagonal parameters  $\eta_{e\mu}$  and  $\eta_{e\tau}$ , it will be sufficient to minimize  $\Delta m_{31}^2$  within its current  $3\sigma$  range to obtain the correct upper bounds on these parameters. For the parameter  $\eta_{e\tau}$ , we observe two disjoint regions, which we will discuss in the next paragraph. The scenario is slightly interesting for  $\eta_{\mu\tau}$ . For this parameter, we obtain an open ended contour, implying that for this parameter, SNSI can mimic the standard scenario with a value of  $\Delta m_{31}^2$  outside its current  $3\sigma$  values. However, we checked that the change in the sensitivity while estimating the upper bounds in both the cases i.e., when  $\Delta m_{31}^2$  is minimized within its  $3\sigma$  values vs the case when  $\Delta m_{31}^2$  minimized with a flat prior, very similar. For this reason, we have chosen to vary this parameter within its  $3\sigma$  values throughout our analysis.

In the top row of Fig.2, we have shown the sensitivity limits on the off-diagonal SNSI parameters for both P2SO and DUNE experiments. In each panel, the red curve represents the sensitivity for DUNE experiment while green curve is for P2SO. The horizontal black solid line corresponds to the benchmark of 90% C.L. From the panels, we see that the bound

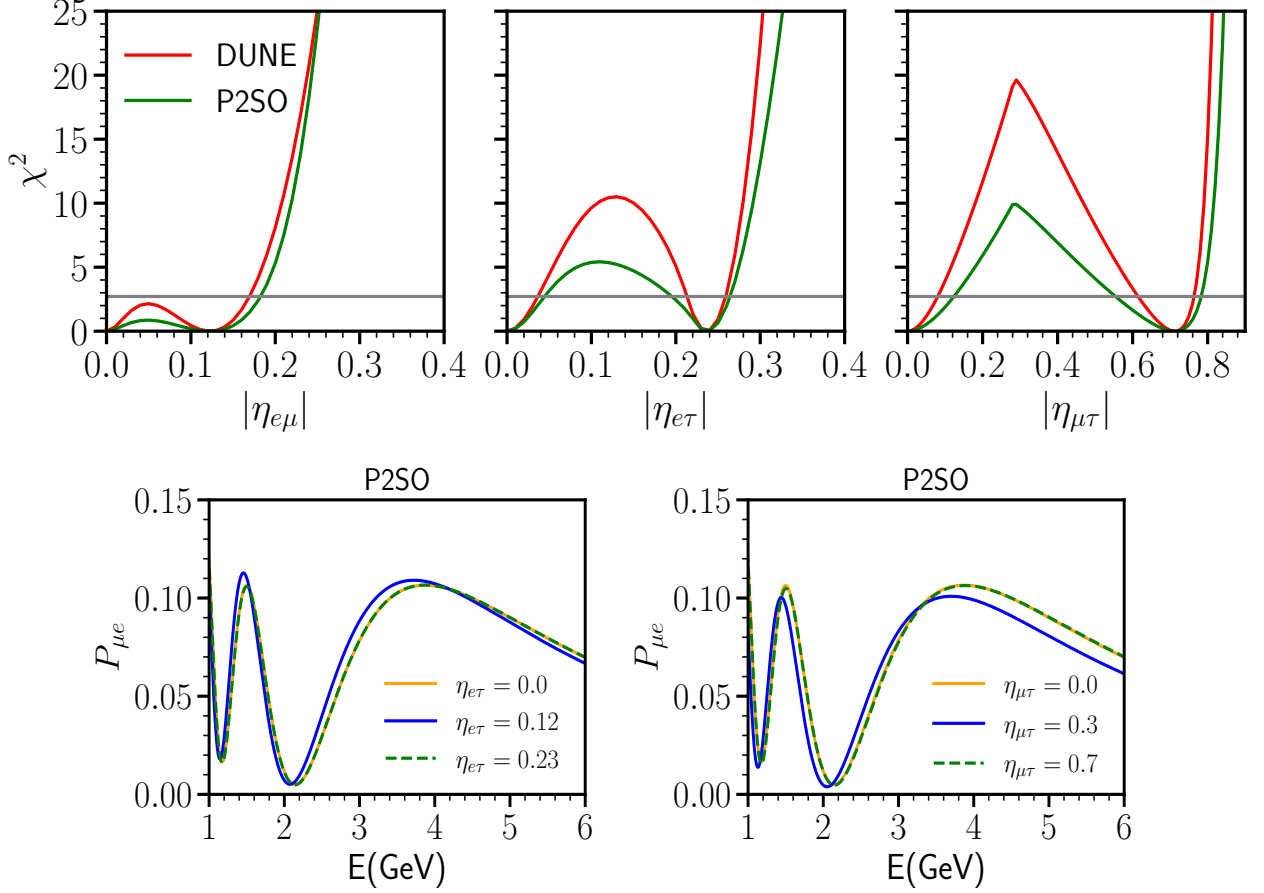


FIG. 2: Top row: Sensitivity limit on the SNSI parameters for P2SO and DUNE experiments. Bottom row: Appearance probability as a function of energy in P2SO for three different cases.

on  $\eta_{e\mu}$  is stronger than  $\eta_{e\tau}$  and the bound on  $\eta_{\mu\tau}$  is weakest among all. The sensitivities of DUNE and P2SO are very similar. It is very interesting to note that all these three off-diagonal parameters mimic the standard scenario even when they assume non-zero values. For  $\eta_{e\mu}/\eta_{e\tau}/\eta_{\mu\tau}$  this degeneracy appears at 0.12/0.23/0.7. The disjoint contour for  $\eta_{e\tau}$  in Fig. 1 appears because of this degeneracy. This degeneracy can be clearly understood from the lower panels where we have shown the appearance channel probability as a function of energy  $E$  for P2SO. Left panel is for  $\eta_{e\tau}$  and the right panel is for  $\eta_{\mu\tau}$ . The orange curve corresponds to the standard scenario and the green dashed curve corresponds to the value of the SNSI parameters for which the degeneracy occurs. The degeneracy is reflected by the fact that these two curves are completely overlapping. The blue curve, where there is no degeneracy, is separated from the other two curves. Similar results can be obtained for the DUNE experiment also.

To understand the role of the phases of the off-diagonal SNSI parameters, we have shown the upper bounds in the  $|\eta_{\alpha\beta}| - \phi_{\alpha\beta}$  plane at 90% C.L. in Fig.3. In each panel, the red (green)



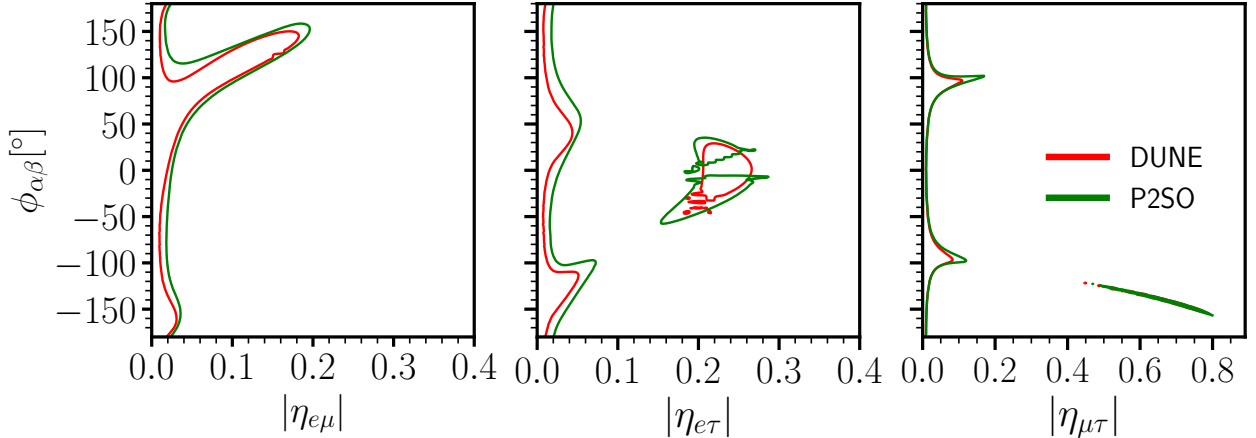


FIG. 3: Allowed parameter space between SNSI parameter  $|\eta_{\alpha\beta}| - \phi_{\alpha\beta}$  plane for P2SO and DUNE experiments at 90% C.L.

SNSI parameter	DUNE		P2SO	
	Value	Phase ( $\phi$ )	Value	Phase ( $\phi$ )
$\eta_{e\mu}$	0.18	$146^\circ$	0.19	$153^\circ$
$\eta_{e\tau}$	0.27	$1.4^\circ$	0.29	$-6.8^\circ$
$\eta_{\mu\tau}$	0.77	$-152.6^\circ$	0.8	$-156.6^\circ$

TABLE II: Sensitivity limits on the SNSI parameters at 90% C.L. from DUNE and P2SO experiments.

coloured contour is the allowed parameter space for DUNE (P2SO) experiment. In these panels, the degeneracies which we see in Figs. 1 and 2 are also visible. From these panels we understand that the sensitivity of the off-diagonal parameters depends on the values of the phases. For example, in the case of  $\eta_{e\mu}$ , the sensitivity is weak around  $\phi_{e\mu} = 146^\circ$ , where we obtain our upper bound. However, if  $\phi_{e\mu}$  happens to be around  $0^\circ$ , then the upper bound of  $\eta_{e\mu}$  will be much stronger. In table II, we have listed the upper bounds of the off-diagonal SNSI parameters and their corresponding values of the phases which we obtained from DUNE and P2SO.

### B. Mass ordering sensitivity

Fig. 4 displays the variation of mass ordering sensitivity as a function of true  $|\eta_{\alpha\beta}|$ . The left/middle/right panel shows the mass ordering sensitivities for the SNSI parameters  $\eta_{e\mu}/\eta_{e\tau}/\eta_{\mu\tau}$ . The red (green) curve represents the sensitivity for the DUNE (P2SO) experiment. Solid (dashed) curves are for  $\phi = 0^\circ(-90^\circ)$ . The experiment's ability to reject the wrong mass ordering when determining the true mass hierarchy is shown in these panels.

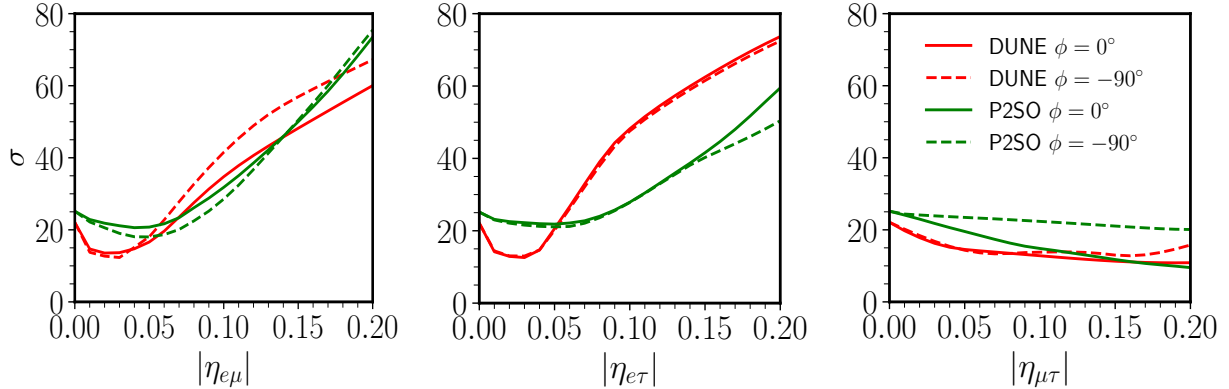


FIG. 4: Variation of mass ordering sensitivity as a function of  $\eta_{\alpha\beta}$  for DUNE and P2SO experiments for different value of true phases.

The behaviour of the curves with respect to  $\eta$  is almost similar for the cases  $\eta_{e\mu}$  and  $\eta_{e\tau}$ . As  $\eta$  increases, the sensitivity initially decreases and then it increases. For  $\eta_{\mu\tau}$ , the sensitivity decreases continuously. The behaviour is similar for both DUNE and P2SO.

To understand the behaviour of the mass ordering curves in Fig. 5, we tried to look at the effect of minimization of the different oscillation parameters. In this figure, the left, middle and right panels are the sensitivities in presence of  $\eta_{e\mu}$ ,  $\eta_{e\tau}$  and  $\eta_{\mu\tau}$ , respectively. In each panel, the orange curve is the scenario when minimization is done over all the oscillation parameters, while the magenta curve is the scenario without any minimization over any parameters. The blue/brown/green curve is obtained with minimizing over only  $\delta_{CP}/\theta_{23}/\phi_{\alpha\beta}$ . This figure provides some important insights. For  $\eta_{\mu\tau}$ , if  $\phi_{\mu\tau}$  is not minimized in the test, then the behaviour of the curve will be the same as  $\eta_{e\mu}$  and  $\eta_{e\tau}$  i.e., sensitivity will first decrease as  $\eta_{\mu\tau}$  increases and then it will increase. In this case, because of the degeneracy with  $\phi$ , the behaviour of the curve gets changed. For  $\eta_{e\mu}$ , we see that even when all the parameters are fixed, the behaviour of the curve remains the same, reflecting the fact that this behaviour does not arise due to the parameter degeneracy. For  $\eta_{e\tau}$ , one can see the effect of degeneracies associated with  $\phi_{e\tau}$  and  $\delta_{CP}$ .

### C. CP violation sensitivity

In Fig 6, we have shown CP violation (CPV) sensitivity for all possible true values of SNSI parameters  $\eta_{\alpha\beta}$  and  $\phi_{\alpha\beta}$ . The upper (lower) panel is for DUNE (P2SO) experiment. CP violation sensitivity signifies the ability to exclude the CP conserving values of  $\delta_{CP}$ . Here, we have considered the maximum CP violation scenario for true  $\delta_{CP} = -90^\circ$ . The color shades in each panel shows the CPV sensitivity in terms of  $\sqrt{\chi^2}$ . It is very interesting to see that in the presence of all three off-diagonal SNSI parameters, the CP sensitivity of both the experiments can become extremely small. This is reflected by the combinations of

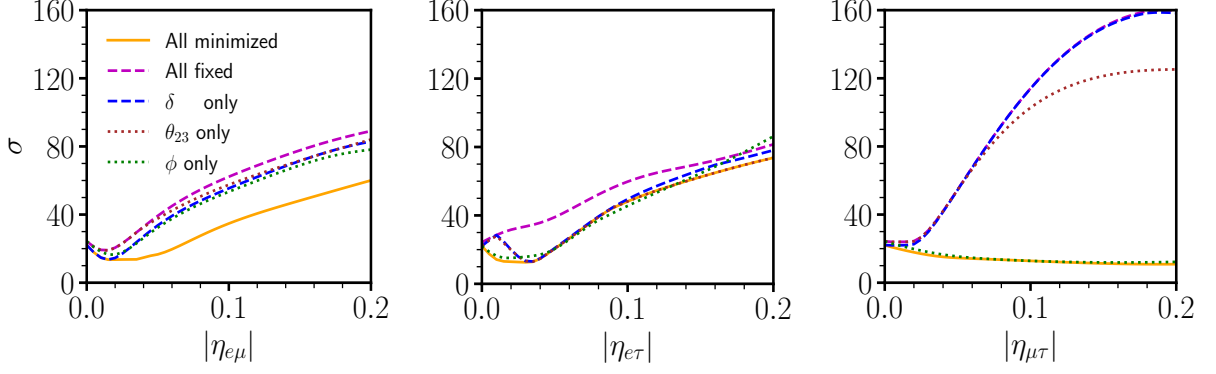


FIG. 5: Variation of mass ordering sensitivity as a function of  $\eta_{\alpha\beta}$  with different minimization conditions over parameters for  $\phi_{true} = 0^\circ$  considering DUNE experiment.

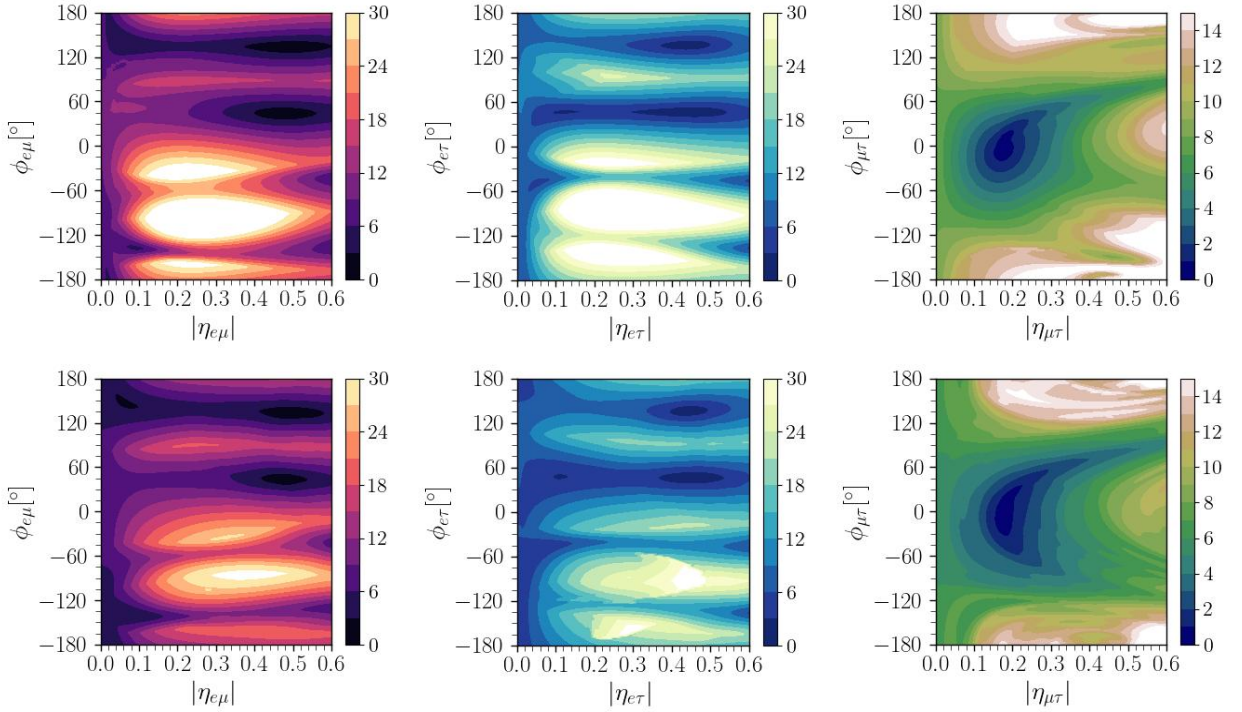


FIG. 6: CP violation sensitivity as a function of  $\eta_{\alpha\beta}$  and  $\phi_{\alpha\beta}$  for DUNE(upper) and P2SO(lower) experiments.

$|\eta_{\alpha\beta}| - \phi_{\alpha\beta}$  for which we obtain the dark black regions. Table III shows the values of  $\eta_{\alpha\beta}$  and  $\phi_{\alpha\beta}$  for which the CP sensitivities of both experiments are completely lost.

#### D. Octant sensitivity

Fig. 7 shows the octant sensitivity as a function of  $\eta_{\alpha\beta}$  for the DUNE and P2SO experiments. Octant sensitivity signifies the capability of the experiments to exclude the possibility

SNSI parameter	DUNE		P2SO	
	Value	Phase( $\phi$ )	Value	Phase( $\phi$ )
$\eta_{e\mu}$	0.47	44°	0.47	44°
$\eta_{e\tau}$	0.48	46°	0.45	46°
$\eta_{\mu\tau}$	0.18	6°	0.18	8°

TABLE III: Values of SNSI parameters at which CP sensitivity is lost.

of wrong octant of  $\theta_{23}$ . We have obtained the sensitivity by taking into account the true octant of  $\theta_{23}$  in LO and HO in the test hypothesis. In the left/middle/right panel, we have shown the octant sensitivity in presence of  $\eta_{e\mu}/\eta_{e\tau}/\eta_{\mu\tau}$  and red (green) curves are for DUNE (P2SO) experiment. In these panels, very interesting characteristics can be observed for every SNSI parameter. For the parameters  $\eta_{e\mu}$  and  $\eta_{e\tau}$ , the sensitivity fluctuates until  $\eta = 0.4$ , after that as  $\eta$  increases, sensitivity increases. For  $\eta_{\mu\tau}$ , a kink in the sensitivity can be observed around  $\eta = 0.6$ . These behaviours of the curves can be explained in a similar fashion as that of Fig. 5.

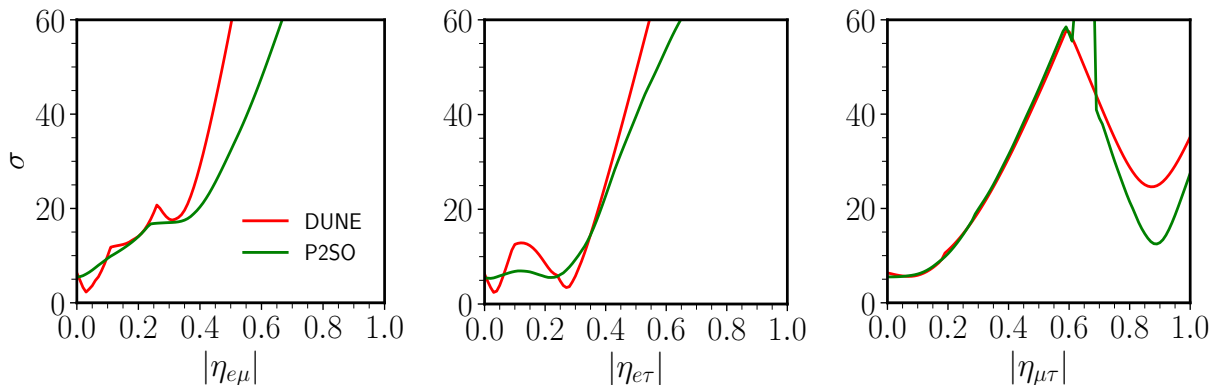


FIG. 7: Octant sensitivity as a function of  $|\eta_{\alpha\beta}|$  for DUNE and P2SO experiment. Here, the true octant considered to be in LO.

### E. Precision of $\theta_{23}$ and $\Delta m_{31}^2$

In this section, we have tried to show the effect of SNSI parameters on the precision measurement of  $\sin^2 \theta_{23}$  and  $\Delta m_{31}^2$ . Fig. 8, shows the allowed parameter space between  $\sin^2 \theta_{23}$  and  $\Delta m_{31}^2$  in the presence of SNSI parameters as well as in the standard interaction case. Left/middle/right panel is for  $\eta_{e\mu}/\eta_{e\tau}/\eta_{\mu\tau}$ . In the left and the middle panels, the values of  $\Delta m_{31}^2$  in the y-axis corresponds to the current  $3\sigma$  values of this parameters. In the right panel, this is shown by the region between the black dotted horizontal lines. In each panel, solid and dashed contours are for DUNE and P2SO, respectively. The red contour represents

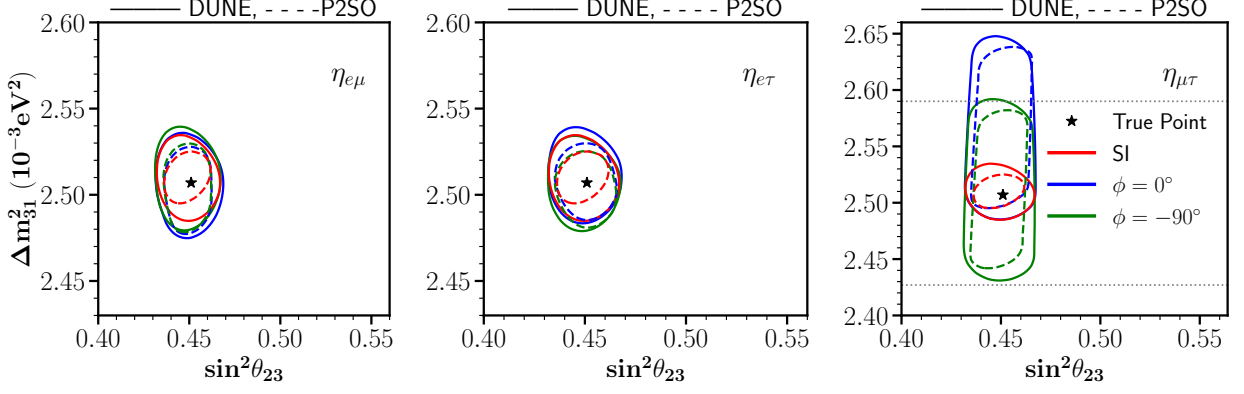


FIG. 8: Allowed parameter space between  $\sin^2 \theta_{23}$ - $\Delta m_{31}^2$  plane for DUNE and P2SO experiments at  $3\sigma$  C.L.

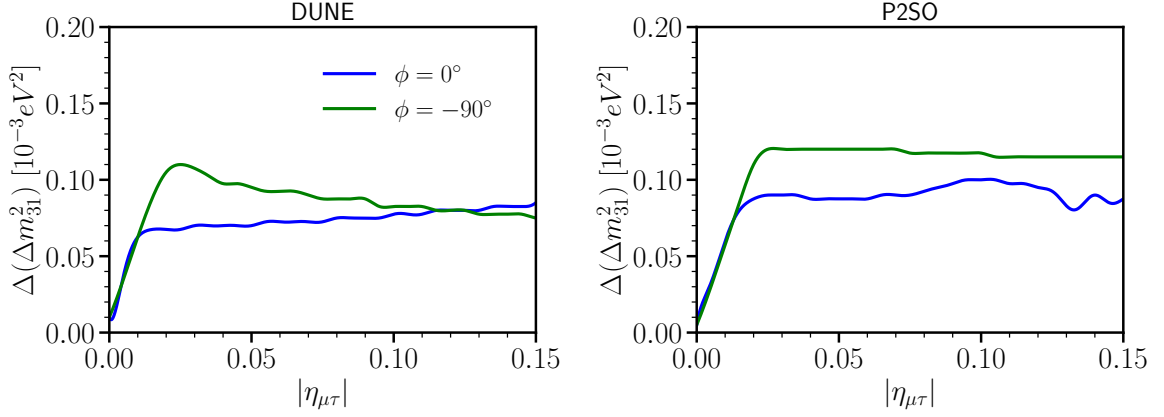


FIG. 9:  $\Delta m_{31}^2$  precision sensitivity at  $1\sigma$  C.L. as a function of  $\eta_{\mu\tau}$  for DUNE and P2SO experiment. We have shown for two different values of  $\phi_{\mu\tau}$ .

the allowed region in SI case, while the green/blue contour symbolises the allowed region for the true value of  $\phi_{\alpha\beta}$  as  $-90^\circ/0^\circ$ . We have considered a benchmark value  $\eta_{\alpha\beta}=0.01$  in both the true and the test scenario for all the cases of  $|\eta_{\alpha\beta}|$ . The true point is represented by the black star in each plot. In the presence of SNSI parameters, the allowed parameter space increases in size compared to the SI case, which implies that the precision of these parameters will get worsen in the presence of SNSI. The deterioration of sensitivity is not so significant in the presence of  $\eta_{e\mu}$  and  $\eta_{e\tau}$ . In both cases the allowed regions are close to the SI contour and within the  $3\sigma$  allowed values of  $\Delta m_{31}^2$  and  $\sin^2 \theta_{23}$ . However, in the case of  $\eta_{\mu\tau}$ , there is a substantial reduction in sensitivity for the precision of  $\Delta m_{31}^2$ . For  $\phi_{\mu\tau} = 0^\circ$ , the allowed region extends beyond the current  $3\sigma$  range of  $\Delta m_{31}^2$ .

To see how the precision of  $\Delta m_{31}^2$  changes for different values  $\eta_{\mu\tau}$ , we have shown the  $1\sigma$  error of  $\Delta m_{31}^2$  in Fig. 9 as a function of  $|\eta_{\mu\tau}|$ . In each panel, the blue curve presents the CP conserving value of  $\phi_{\mu\tau} = 0^\circ$ , while the green curve represents the precision plot for

maximum CP violating value of  $\phi_{\mu\tau}$  as  $-90^\circ$ . From the panels, we see that as  $\eta_{\mu\tau}$  increases from zero, the precision of  $\Delta m_{31}^2$  decreases. For higher values of  $\eta_{\mu\tau}$ , the precision of  $\Delta m_{31}^2$  remains constant.

## V. SUMMARY AND CONCLUSION

In this paper, we have studied the impact of the off-diagonal SNSI parameters in the future long-baseline experiments DUNE and P2SO. In our analysis, we have found that unlike in the diagonal SNSI parameters, the parameter  $\Delta m_{31}^2$  does not play any non-trivial role when one tries to put bounds on these parameters. For the parameters  $\eta_{e\mu}$  and  $\eta_{e\tau}$ , SNSI can be fitted with the standard three flavour scenario, with a value of  $\Delta m_{31}^2$  within its current  $3\sigma$  range. For  $\eta_{\mu\tau}$ , though the values of  $\Delta m_{31}^2$  beyond its current  $3\sigma$  range gets allowed, when one tries to fit the standard scenario with SNSI, the impact of  $\Delta m_{31}^2$  is very minimal while estimating the upper bound of this parameter. For all these three off-diagonal parameters, we have identified a degeneracy where the standard three flavour scenario mimics the SNSI scenario even for a non-zero values of  $\eta_{e\mu}$ ,  $\eta_{e\tau}$  and  $\eta_{\mu\tau}$ . We have also found out that the bounds on the SNSI parameters also depend on the phases associated with them. Among the three parameters, the bound on  $\eta_{e\mu}$  is strongest and the bound on  $\eta_{\mu\tau}$  is weakest. The sensitivities of both the experiments are very similar in this regard.

Next we tried to understand how the sensitivities of these experiments get affected if one assumes the off-diagonal SNSI exists in Nature. Regarding the mass ordering sensitivity, we have shown that as  $\eta$  increases from zero, the sensitivity initially increases and then decreases for the parameters  $\eta_{e\mu}$  and  $\eta_{e\tau}$ , whereas for the parameter  $\eta_{\mu\tau}$ , it decreases continuously. We have explained this behaviour from the argument of degeneracies among different parameters. For CP sensitivity, the conclusions for the off-diagonal parameters are very similar as the diagonal parameters i.e., for some combinations of  $|\eta|$  and  $\phi$ , the CP sensitivity of both the experiments can be very small or even they can vanish. As far as octant sensitivity is concerned, for the parameters  $\eta_{e\mu}$  and  $\eta_{e\tau}$ , the sensitivity fluctuates until  $\eta = 0.4$ , after that as  $\eta$  increases, sensitivity increases. For  $\eta_{\mu\tau}$ , a kink in the sensitivity can be observed around  $\eta = 0.6$ . Finally, regarding the precision of the atmospheric mixing parameters  $\Delta m_{31}^2$  and  $\theta_{23}$ , we have found out that in the presence of off-diagonal SNSI, their sensitivity gets worsened as compared to the standard scenario. The effect is more prominent in the case of  $\eta_{\mu\tau}$  for which the precision of  $\Delta m_{31}^2$  deteriorates significantly.

In conclusion, we would like to emphasize that if a non-zero off-diagonal SNSI exists in nature, it will alter the phenomenology of the long-baseline experiments in a very non-trivial way. For example, depending on the values of these parameters, they can either completely mimic the standard scenario or can wash out their CP sensitivity. Therefore, it is very important to look for the existence of this theory in the current and future data of the neutrino oscillation experiments.

## ACKNOWLEDGEMENTS

SKP would like to acknowledge University Grants Commission for the NFOBC fellowship. DKS would like to acknowledge Prime Minister's Research Fellowship, Govt. of India. This work has been in part funded by Ministry of Science and Education of Republic of Croatia grant No. KK.01.1.1.01.0001. RM acknowledges the support from University of Hyderabad through IoE project grant no. RC1-20-012.

---

- [1] I. Esteban, M. C. Gonzalez-Garcia, M. Maltoni, T. Schwetz, and A. Zhou, *JHEP* **09**, 178 (2020), arXiv:2007.14792 [hep-ph].
- [2] I. Esteban, M. C. Gonzalez-Garcia, M. Maltoni, I. Martinez-Soler, J. a. P. Pinheiro, and T. Schwetz, (2024), arXiv:2410.05380 [hep-ph].
- [3] S. Antusch, J. P. Baumann, and E. Fernandez-Martinez, *Nucl. Phys. B* **810**, 369 (2009), arXiv:0807.1003 [hep-ph].
- [4] M. B. Gavela, D. Hernandez, T. Ota, and W. Winter, *Phys. Rev. D* **79**, 013007 (2009), arXiv:0809.3451 [hep-ph].
- [5] T. Ohlsson, *Rept. Prog. Phys.* **76**, 044201 (2013), arXiv:1209.2710 [hep-ph].
- [6] C. Biggio, M. Blennow, and E. Fernandez-Martinez, *JHEP* **08**, 090 (2009), arXiv:0907.0097 [hep-ph].
- [7] Y. Farzan and M. Tortola, *Front. in Phys.* **6**, 10 (2018), arXiv:1710.09360 [hep-ph].
- [8] O. W. Greenberg, *Phys. Rev. Lett.* **89**, 231602 (2002), arXiv:hep-ph/0201258.
- [9] V. A. Kostelecky and M. Mewes, *Phys. Rev. D* **69**, 016005 (2004), arXiv:hep-ph/0309025.
- [10] T. Katori (MiniBooNE), *Mod. Phys. Lett. A* **27**, 1230024 (2012), arXiv:1206.6915 [hep-ex].
- [11] J. S. Diaz, *Adv. High Energy Phys.* **2014**, 962410 (2014), arXiv:1406.6838 [hep-ph].
- [12] A. S. Joshipura and S. Mohanty, *Phys. Lett. B* **584**, 103 (2004), arXiv:hep-ph/0310210.
- [13] J. A. Grifols and E. Masso, *Phys. Lett. B* **579**, 123 (2004), arXiv:hep-ph/0311141.
- [14] M. C. Gonzalez-Garcia, P. C. de Holanda, E. Masso, and R. Zukanovich Funchal, *JCAP* **01**, 005 (2007), arXiv:hep-ph/0609094.
- [15] J. N. Bahcall, N. Cabibbo, and A. Yahil, *Phys. Rev. Lett.* **28**, 316 (1972).
- [16] M. Lindner, T. Ohlsson, and W. Winter, *Nucl. Phys. B* **607**, 326 (2001), arXiv:hep-ph/0103170.
- [17] J. F. Beacom and N. F. Bell, *Phys. Rev. D* **65**, 113009 (2002), arXiv:hep-ph/0204111.
- [18] A. Bandyopadhyay, S. Choubey, and S. Goswami, *Phys. Lett. B* **555**, 33 (2003), arXiv:hep-ph/0204173.
- [19] A. S. Joshipura, E. Masso, and S. Mohanty, *Phys. Rev. D* **66**, 113008 (2002), arXiv:hep-ph/0203181.

- [20] G. Barenboim, N. E. Mavromatos, S. Sarkar, and A. Waldron-Lauda, Nucl. Phys. B **758**, 90 (2006), arXiv:hep-ph/0603028.
- [21] E. Lisi, A. Marrone, and D. Montanino, Phys. Rev. Lett. **85**, 1166 (2000), arXiv:hep-ph/0002053.
- [22] G. L. Fogli, E. Lisi, A. Marrone, D. Montanino, and A. Palazzo, Phys. Rev. D **76**, 033006 (2007), arXiv:0704.2568 [hep-ph].
- [23] M. M. Guzzo, P. C. de Holanda, and R. L. N. Oliveira, Nucl. Phys. B **908**, 408 (2016), arXiv:1408.0823 [hep-ph].
- [24] Y. Grossman, Phys. Lett. B **359**, 141 (1995), arXiv:hep-ph/9507344.
- [25] V. D. Barger, R. J. N. Phillips, and K. Whisnant, Phys. Rev. D **44**, 1629 (1991).
- [26] S.-F. Ge and S. J. Parke, Phys. Rev. Lett. **122**, 211801 (2019), arXiv:1812.08376 [hep-ph].
- [27] S.-F. Ge and H. Murayama, (2019), arXiv:1904.02518 [hep-ph].
- [28] P. B. Denton, A. Giarnetti, and D. Meloni, JHEP **02**, 210 (2023), arXiv:2210.00109 [hep-ph].
- [29] R. Cordero, L. A. Delgadillo, and O. G. Miranda, Phys. Rev. D **107**, 075023 (2023), arXiv:2207.11308 [hep-ph].
- [30] A. Gupta, D. Majumdar, and S. Prakash, (2023), arXiv:2306.07343 [hep-ph].
- [31] A. Medhi, D. Dutta, and M. M. Devi, JHEP **06**, 129 (2022), arXiv:2111.12943 [hep-ph].
- [32] A. Medhi, M. M. Devi, and D. Dutta, JHEP **01**, 079 (2023), arXiv:2209.05287 [hep-ph].
- [33] A. Medhi, A. Sarker, and M. M. Devi, (2023), arXiv:2307.05348 [hep-ph].
- [34] T. Sarkar, (2022), arXiv:2209.10233 [hep-ph].
- [35] K. S. Babu, G. Chauhan, and P. S. Bhupal Dev, Phys. Rev. D **101**, 095029 (2020), arXiv:1912.13488 [hep-ph].
- [36] D. K. Singha, R. Majhi, L. Panda, M. Ghosh, and R. Mohanta, (2023), arXiv:2308.10789 [hep-ph].
- [37] B. Dutta, S. Ghosh, K. J. Kelly, T. Li, A. Thompson, and A. Verma, (2024), arXiv:2401.02107 [hep-ph].
- [38] J. Aguilar *et al.* (ESSnuSB), Phys. Rev. D **109**, 115010 (2024), arXiv:2310.10749 [hep-ex].
- [39] A. Sarker, A. Medhi, D. Bezboruah, M. M. Devi, and D. Dutta, (2023), arXiv:2309.12249 [hep-ph].
- [40] A. Sarker, D. Bezboruah, A. Medhi, and M. M. Devi, (2024), arXiv:2406.15307 [hep-ph].
- [41] P. B. Denton, A. Giarnetti, and D. Meloni, (2024), arXiv:2409.15411 [hep-ph].
- [42] D. Bezboruah, D. S. Chattopadhyay, A. Medhi, A. Sarker, and M. M. Devi, (2024), arXiv:2410.05250 [hep-ph].
- [43] B. Dutta, S. Ghosh, T. Li, A. Thompson, and A. Verma, JHEP **03**, 163 (2023), arXiv:2209.13566 [hep-ph].
- [44] A. V. Akhondinov *et al.*, Eur. Phys. J. C **79**, 758 (2019), arXiv:1902.06083 [physics.ins-det].
- [45] D. K. Singha, M. Ghosh, R. Majhi, and R. Mohanta, Phys. Rev. D **107**, 075039 (2023), arXiv:2211.01816 [hep-ph].



- [46] R. Majhi, D. K. Singha, M. Ghosh, and R. Mohanta, *Phys. Rev. D* **107**, 075036 (2023), arXiv:2212.07244 [hep-ph].
- [47] B. Abi *et al.* (DUNE), (2021), arXiv:2103.04797 [hep-ex].
- [48] P. Huber, M. Lindner, and W. Winter, *Comput. Phys. Commun.* **167**, 195 (2005), arXiv:hep-ph/0407333.
- [49] P. Huber, J. Kopp, M. Lindner, M. Rolinec, and W. Winter, *Comput. Phys. Commun.* **177**, 432 (2007), arXiv:hep-ph/0701187.
- [50] G. L. Fogli, E. Lisi, A. Marrone, D. Montanino, and A. Palazzo, *Phys. Rev. D* **66**, 053010 (2002), arXiv:hep-ph/0206162.
- [51] P. Huber, M. Lindner, and W. Winter, *Nucl. Phys. B* **645**, 3 (2002), arXiv:hep-ph/0204352.